Copy
RM L53I11

NACA

RESEARCH MEMORANDUM

FOR REFERENCE

NOT TO BE TAKEN FROM THIS ROOM

FREE-FLIGHT-TUNNEL INVESTIGATION OF THE LOW-SPEED STABILITY AND CONTROL CHARACTERISTICS OF A CANARD AIRPLANE MODEL

By Joseph L. Johnson, Jr., and John W. Paulson

Langley Aeronautical Laboratory
Langley Field, Va.

NATIONAL ADVISORY COMMITTEE
FOR AERONAUTICS

WASHINGTON
October 29, 1953

NATIONAL ADVISORY COMMITTEE FOR AERONAUTICS

RESEARCH MEMORANDUM

FREE-FLIGHT-TUNNEL INVESTIGATION OF THE LOW-SPEED STABILITY AND CONTROL CHARACTERISTICS OF A CANARD AIRPLANE MODEL

By Joseph L. Johnson, Jr., and John W. Paulson

SUMMARY

Since canard configurations have been found to possess unusual static stability characteristics, an investigation has been conducted in the Langley free-flight tunnel to determine the dynamic stability and control characteristics of a model of this type. The characteristics of the model were unsatisfactory in the higher lift-coefficient range because of lightly damped lateral oscillations and because of erratic behavior in pitch and yaw which was apparently caused by random trim changes associated with the irregular fluctuations in the vortex flow from the horizontal tail.

INTRODUCTION

During the past few years the National Advisory Committee for Aeronautics has been making a general study of canard airplanes because they appear to offer some advantages over other type airplanes at transonic and supersonic speeds (for example, refs. 1 to 3). As a part of this general study, several investigations have been conducted in the Langley free-flight tunnel to determine the low-speed static longitudinal and lateral stability and control characteristics of canard airplane models (refs. 4 to 9). The longitudinal studies showed that the particular canard designs studied had a relatively small allowable center-of-gravity range unless the trimming power of the tail was increased by increasing the maximum lift coefficient of the tail (ref. 9). The lateral studies showed that, at high angles of attack, a sidewash from the horizontal tail caused an effective reversal in the direction of sideslip which resulted in the models having large positive values of directional stability with vertical tails off. This sidewash also caused the directional stability contributed by a vertical tail on the fuselage to be reduced at high angles of attack. An investigation to determine the damping-in-yaw characteristics

of a particular canard model (ref. 7) showed that the sidewash caused the model to have negative damping in yaw with vertical tails off and caused the damping-in-yaw contribution of a vertical tail at the rear of the fuselage to be increased.

Because of the unusual nature of these stability characteristics, an investigation was undertaken to flight test a canard model in the Langley free-flight tunnel in order to determine the effect of these characteristics on dynamic stability and control and general flying qualities. Flight tests were made of the model over a lift-coefficient range from about 0.55 to the stall with various vertical tail arrangements. For most of the tests a 60° triangular-plan-form horizontal tail was used on the model but for some tests the 45° sweptback tail with leading-edge flap investigated in reference 9 was used. Calculations were made to determine the dynamic lateral stability characteristics of the model for correlation with flight-test results.

SYMBOLS

All forces and moments are referred to the stability system of axes originating at a center-of-gravity position of $0.24\bar{c}$ ahead of the leading edge of the mean aerodynamic chord and vertically on the center line of the model. A sketch showing the positive direction of the forces and moments is presented in figure 1 and the relation of the stability axes to the other axes considered herein is shown in figure 2.

S	wing area, sq ft
$\bar{c}$	mean aerodynamic chord, ft
V	airspeed, ft/sec
b	wing span, ft
q	dynamic pressure, lb/sq ft
ρ	air density, slugs/cu ft
W	weight, lb
m	mass, slugs
μ_b	relative density factor, $m/\rho Sb$
β	angle of sideslip, deg

α	angle of attack of reference axis (fig. 1), deg
η	angle of attack of principal longitudinal axis of airplane, positive when principal axis is above flight path at nose (fig. 2), deg
ϵ	angle between reference axis and principal axis, positive when reference axis is above principal axis at nose (fig. 2), deg
θ	angle between reference axis and horizontal axis, positive when reference axis is above horizontal axis at nose (fig. 2), deg
γ	angle of flight to horizontal axis, positive in a climb (fig. 2), deg
I_X	moment of inertia about reference longitudinal axis, mk_X^2, slug-ft^2
I_Y	moment of inertia about reference lateral axis, mk_Y^2, slug-ft^2
I_Z	moment of inertia about reference vertical axis, mk_Z^2, slug-ft^2
k_{X_o}	radius of gyration about principal longitudinal axis, ft
k_{Z_o}	radius of gyration about principal vertical axis, ft
k_X	radius of gyration about reference longitudinal axis, ft
k_Y	radius of gyration about reference lateral axis, ft
k_Z	radius of gyration about reference vertical axis, ft
K_{X_o}	nondimensional radius of gyration about principal longitudinal axis, k_{X_o}/b
K_{Z_o}	nondimensional radius of gyration about principal vertical axis, k_{Z_o}/b

K_X nondimensional radius of gyration about longitudinal stability axis, $\sqrt{K_{X_o}{}^2\cos^2\eta + K_{Z_o}{}^2\sin^2\eta}$

K_Z nondimensional radius of gyration about vertical stability axis, $\sqrt{K_{Z_o}{}^2\cos^2\eta + K_{X_o}{}^2\sin^2\eta}$

K_{XZ} nondimensional product-of-inertia parameters, $\left(K_{Z_o}{}^2 - K_{X_o}{}^2\right)\cos\eta \sin\eta$

C_L lift coefficient, Lift/qS

C_D drag coefficient, Drag/qS

C_m pitching-moment coefficient, Pitching moment/qS$\bar{c}$

C_n yawing-moment coefficient, Yawing moment/qSb

C_l rolling-moment coefficient, Rolling moment/qSb

C_Y lateral-force coefficient, Lateral force/qS

$C_{Y_\beta} = \frac{\partial C_Y}{\partial \beta}$, per degree (per radian in table II)

$C_{n_\beta} = \frac{\partial C_n}{\partial \beta}$, per degree (per radian in table II)

$C_{l_\beta} = \frac{\partial C_l}{\partial \beta}$, per degree (per radian in table II)

$C_{Y_p} = \frac{\partial C_Y}{\partial \frac{pb}{2V}}$, per radian

$C_{l_p} = \frac{\partial C_l}{\partial \frac{pb}{2V}}$, per radian

$C_{n_p} = \frac{\partial C_n}{\partial \frac{pb}{2V}}$, per radian

$C_{l_r} = \frac{\partial C_l}{\partial \frac{rb}{2V}}$, per radian

$C_{Y_r} = \frac{\partial C_Y}{\partial \frac{rb}{2V}}$, per radian

$C_{n_r} = \frac{\partial C_n}{\partial \frac{rb}{2V}}$, per radian

i_t incidence of horizontal tail (positive with leading edge up), deg

δ_a aileron deflection perpendicular to hinge line, deg

p rolling angular velocity, radians/sec

r yawing angular velocity, radians/sec

$T_{1/2}$ time for amplitude of oscillation to change by factor of 2 (positive value indicates a decrease to half-amplitude; negative value indicates an increase to double amplitude), sec

APPARATUS AND MODEL

The investigation was conducted in the Langley free-flight tunnel which is designed to test free-flying dynamic models. A complete description of the tunnel and its operation is presented in reference 10. The free-oscillation tests to determine the damping-in-yaw characteristics of the flight-test model were made in the Langley free-flight tunnel during a previous investigation (ref. 7). The rolling derivatives of the flight-test model were determined by the rolling flow method of the Langley stability tunnel which is described in reference 11.

The model used in the investigation was constructed at the Langley Laboratory. A three-view drawing of the model is presented in figure 3

and the dimensional and mass characteristics of the model are given in table I. A photograph of the model with the all-movable triangular horizontal tail and wing-tip vertical tails is shown in figure 4. The model was equipped with wing-tip tails in its basic condition. For some tests the model was equipped with a center vertical tail on the rear of the fuselage and also with the center vertical tail in combination with the wing-tip tails.

The center-of-gravity position of the model could be varied about 14 percent of the mean aerodynamic chord during flight by moving a weight along the longitudinal axis of the fuselage. A 1-inch movement of the weight gave approximately a 1-percent shift in the center-of-gravity position.

DETERMINATION OF THE STATIC STABILITY AND CONTROL AND ROTARY CHARACTERISTICS OF THE FLIGHT-TEST MODEL

Test Conditions

Force tests were made to determine the static longitudinal and lateral stability and control characteristics of the model with tip tails on over an angle-of-attack range from 0° to 32° with the triangular horizontal tail and with the sweptback horizontal tail. The lateral characteristics were also determined for each horizontal tail configuration with all vertical tails off, with wing-tip tails alone, with center tail alone, and with center tail plus wing-tip tails. The lateral characteristics were determined from measurements of force and moment coefficients at $\pm 5^\circ$ sideslip and over a yaw range of $\pm 20^\circ$ at angles of attack of 0°, 12°, 16°, and 24°. Most of the tests were made with the elevons deflected -15° and the horizontal tail deflected 5° which corresponded to those deflections used for trim in most of the flight tests.

All force tests were made at a dynamic pressure of 3.0 pounds per square foot which corresponds to an airspeed of about 50 feet per second at standard sea-level conditions and to a Reynolds number of approximately 0.443×10^6 based on the wing mean aerodynamic chord of 1.38 feet. All moment data are referred to a center-of-gravity position of 24.0 percent of the mean aerodynamic chord ahead of the leading edge of the mean aerodynamic chord.

Damping-in-yaw tests (reported in ref. 7) were made over an angle-of-attack range from 0° to 20° with tip tails off and on. Tests were also made at an angle of attack of 20° with wing-tip tails and a center vertical tail on the fuselage. These tests were run at a dynamic pressure

of 1.2 pounds per square foot which corresponds to an airspeed of approximately 31 feet per second and to a Reynolds number of 0.275×10^6 based on the mean aerodynamic chord of the wing.

The rolling-flow tests were made over an angle-of-attack range from 0° to 28° for the model with all vertical tails off, with wing-tip tails only, with center tail only, and also with wing-tip tails plus center tail. These tests were made at a dynamic pressure of 16 pounds per square foot which corresponds to an airspeed of approximately 116 feet per second and to a Reynolds number of 1.02×10^6 based on the mean aerodynamic chord of the wing.

Longitudinal Stability and Control

The data of figure 5 show the effect of horizontal-tail deflection on the static longitudinal stability and control characteristics of the model with the triangular horizontal tail and with the sweptback horizontal tail having a leading-edge flap. The data show similar characteristics for the two configurations although there was generally less stability and more pitching effectiveness with the sweptback tail because of its greater lift-curve slope. Both tails lost their effectiveness when the combined angle of attack of the model and angle of incidence of the tail equalled the stall angle of the tail.

The effects on the longitudinal stability and control characteristics of deflecting the ailerons for trim (both ailerons deflected up 15°) are shown in figure 6. Deflection of the ailerons produced a constant increment of positive pitching-moment coefficient throughout the lift-coefficient range which increased the trim lift coefficient for both configurations.

Lateral Stability and Control

The effect of vertical-tail arrangement on the lateral stability characteristics of the model at various angles of attack with the triangular horizontal tail and with the sweptback horizontal tail plus flap are shown in figures 7 and 8, respectively. Since the variation of yawing-moment coefficient C_n with angle of sideslip β is nonlinear for some configurations, the yawing-moment data of figures 7 and 8 are summarized in figure 9 in terms of the directional stability parameter C_{n_β} as measured at low angles of sideslip ($\beta < \pm 5^\circ$) and high angles of sideslip ($\beta > \pm 5^\circ$). The data show that the static directional stability of the model was satisfactory over the angle-of-attack range with tip tails on at either low or high sideslip angles. The center tail

[redacted]

was destabilizing at low sideslip angles over the higher angle-of-attack range. This destabilizing effect resulted in large static instability at 24° angle of attack with only the center tail on.

The variation of aileron and rudder effectiveness with angle of attack is presented in figure 10. The rolling moment produced by various amounts of aileron deflection from a neutral setting of -15° decreases with increasing angle of attack. The yawing moment produced by the ailerons is generally adverse over the angle-of-attack range for all deflections. The yawing moment produced by 10° deflection of the wing-tip rudders decreases by about two-thirds from low to high angles of attack but it still appears to be sufficient to balance out the adverse yawing moment produced by the ailerons over the angle-of-attack range. The yawing moment produced by a deflection of 10° of the center rudder plus wing-tip rudders is approximately two and one-half to five times as great as that produced by the tip rudders alone.

Damping-In-Yaw Characteristics

The data of figure 11 show the damping-in-yaw characteristics of the model with the triangular horizontal tail as presented in reference 7. These data show that with vertical tails off or tip tails on the damping decreased and became negative as the angle of attack increased. The addition of the center tail to the model gave a large stabilizing increment to the damping in yaw at 20° angle of attack.

Rolling Derivatives

The results of rolling flow tests to determine the rolling derivatives of the model with the triangular horizontal tail are presented in figure 12. These data show that the damping-in-roll parameter $-C_{l_p}$ decreases with an increase in angle of attack for all vertical tail arrangements tested. The yawing moment due to rolling C_{n_p} was greatly affected by vertical-tail arrangement and angle of attack. With vertical tails off C_{n_p} was negative at low angles of attack but became positive in the medium angle-of-attack range and increased to large positive values at the higher angles of attack. The increment of C_{n_p} contributed by the the wing-tip tails and wing-tip tails plus center tail was positive in the lower angle-of-attack range and negative in the moderate and high angle-of-attack ranges. The lateral force due to rolling C_{Y_p}, which varied considerably with vertical-tail arrangement at the higher angle of attack, was positive over most of the angle-of-attack range for all the vertical-tail arrangements tested.

[redacted]

FLIGHT TESTS

Flight tests were made over a lift-coefficient range from about 0.55 to the stall to determine the dynamic stability and control characteristics of the model with various vertical-tail arrangements. The vertical-tail arrangements tested included wing-tip tails alone, center tail alone, center tail plus wing-tip tails, and all tails off. Most of the flights of the model were made with the triangular horizontal tail but a few flights were made with the sweptback horizontal tail having a leading-edge flap.

In order to keep the incidence of the horizontal tail low and thus avoid tail stall and the resulting loss in effectiveness at high angles of attack, the model was trimmed over the lift-coefficient range by changing the center-of-gravity position of the model. In the investigation the center-of-gravity position was varied from about $0.26\bar{c}$ ahead of the leading edge of the mean aerodynamic chord to about $0.12\bar{c}$ ahead of the leading edge of the mean aerodynamic chord. The model was flown with coordinated ailerons and rudder and also with ailerons alone. Aileron deflections of $\pm 15^\circ$ and $\pm 20^\circ$, rudder deflections up to $\pm 10^\circ$, and horizontal-tail deflections of $\pm 5^\circ$ were used for control during the flight tests.

Motion-picture records were taken throughout the flight tests to supplement the pilots' observations of the behavior of the model.

CALCULATIONS

Calculations were made by the method presented in reference 12 to determine the period and time to damp to one-half amplitude of the lateral oscillatory mode and the time to damp to one-half amplitude of the aperiodic modes for the model with the various vertical-tail configurations investigated.

The aerodynamic and mass characteristics used in the calculations are presented in table II. These values are based on a center-of-gravity position of $0.24\bar{c}$ ahead of the leading edge of the mean aerodynamic chord and are considered representative of all flight conditions since the variation of center-of-gravity position used in the investigation would not greatly affect these factors. Values of C_{Y_β}, C_{n_β}, and C_{l_β} for the model were obtained from force tests made in the free-flight tunnel. (See fig. 9.) The tail-off values of C_{Y_r} and C_{l_r} were estimated from references 12 and 13. The contribution of the vertical tail to the stability derivatives C_{Y_r} and C_{l_r} and, in some cases, C_{n_r} was estimated

from the equations given at the bottom of table II, which are similar to those given in reference 12. Most of the C_{n_r} values for the model were obtained from damping-in-yaw tests made in the free-flight tunnel. (See fig. 11.) Values of C_{Y_p}, C_{n_p}, and C_{l_p} were obtained from the rolling-flow tests made in the stability tunnel (see fig. 12).

RESULTS AND DISCUSSION

For the most part the dynamic stability and control characteristics were evaluated for the model with the triangular horizontal tail, but a few flights were made to determine the effect of the sweptback tail on the model characteristics. Since these tests indicated that there was no appreciable difference in the dynamic characteristics of the model with the two horizontal-tail configurations, the discussion will be concerned specifically with the model having the triangular tail but can be assumed to apply also to the model with the sweptback tail.

Longitudinal Stability and Control

The dynamic longitudinal stability and control characteristics of the model with the triangular horizontal tail were considered satisfactory at the lower lift coefficients tested. The model flew smoothly and the response to elevator control appeared to be satisfactory. As the lift coefficient was increased, however, the behavior of the model became somewhat erratic and the model was more difficult to control. Near the stall the model exhibited longitudinal unsteadiness and was difficult to settle down to a given trim condition. At times when the model appeared to stall, it settled to the tunnel floor without any apparent pitching tendency.

A part of the poor longitudinal behavior at high lift coefficients could be attributed to the low static margin which resulted from the rearward shift in the center-of-gravity position to permit trim at the high lift coefficients. The main factor contributing to the erratic behavior of the model, however, was apparently the random changes in trim brought about by the irregular fluctuations in the vortex flow from the horizontal tail. This vortex flow, as reported in reference 8, was found to have rather large variations in the asymmetrical disposition of the vortices as a result of relatively small changes in sideslip and angle of attack. Since in the present model the angle of incidence of the tail also changed whenever longitudinal control was applied, the fluctuations in the vortex flow over the wing and fuselage were probably exceptionally large and contributed greatly to the overall erratic behavior of the model.

[redacted]

The longitudinal control characteristics of the model were generally satisfactory over the lift-coefficient range providing that trim settings in the order of 5° or less for the horizontal tail were used. With angles of incidence greater than 5°, an angle of attack was reached where deflecting the tail to produce a nose-up pitching moment resulted in the tail stalling and losing its control effectiveness. Under these conditions the model responded very slowly in pitch and it was difficult to control the vertical position of the model in the tunnel. (This decrease in pitching effectiveness of the horizontal tail is shown by the force data of figs. 5 and 6.)

Lateral Stability and Control

Wing-tip vertical tails.- The lateral oscillation was well damped at low lift coefficients and the lateral stability characteristics of the model with wing-tip tails were considered satisfactory. Fairly smooth flights were obtained with coordinated ailerons and rudder or with ailerons alone although there was slightly more yawing with ailerons alone. As the lift coefficient increased, the damping of the lateral oscillation decreased and flights became so erratic that the pilot had to continually control the model in order to maintain flight. This reduction in oscillatory stability with increase in lift coefficient, which is also shown by the calculated results of figure 13, was probably caused by the decrease in damping in yaw (fig. 11). The calculations indicate that the model actually became unstable at high lift coefficients but this result could not be verified in flight tests because of the extremely erratic flight behavior of the model which necessitated the use of almost continual control and thereby tended to mask any instability that might have been present.

Another factor contributing to the generally poor lateral characteristics at high lift coefficients was the fluctuations in the vortex flow previously discussed. The large changes in vortex disposition with angle of sideslip which resulted in changes in damping in yaw and static lateral stability also appeared to cause random trim changes in yaw. The pilot had the feeling in flying this model that he had to be constantly alert to prevent the model from reaching an attitude from which it could not be recovered. This was particularly true during flights with ailerons alone used for control since there was no yaw control available to correct for any out-of-trim yawing moment produced by the ailerons or by the vortex flow. Even with coordinated ailerons and rudder the model would sometimes yaw and stay trimmed at some angle of sideslip for a short time and then perhaps change its angle of sideslip or slide into the tunnel wall with full control being applied in an effort to stop the motion.

Wing-tip tails plus center vertical tails.- With the addition of a center vertical tail it appeared that the damping of the lateral oscillation was increased over that of the model with tip tails on but the lateral oscillation was still only lightly damped at the higher lift coefficients. This increased damping of the lateral oscillation was mainly caused by the large increase in the damping in yaw (fig. 11). The calculated results of figure 13 are in general agreement with the flight tests in that they show a decrease in oscillatory stability as the lift coefficient increased. The calculated increase in oscillatory stability provided by the addition of the center vertical tail, however, was apparently larger than the increase observed in the flight tests.

At high lift coefficients the model still exhibited the erratic flight behavior associated with the vortex flow from the horizontal tail. There was no essential difference in the behavior of the model compared with that of the tip-tail case except that the increased rudder power realized through the addition of the center tail seemed to make recovery from disturbances somewhat easier.

Center vertical tail.- Flight tests of the model with only the center vertical tail indicated that the oscillatory characteristics were about the same as those of the model with tip vertical tails and the model exhibited the same random motions associated with the vortex flow as in the case of the other configurations. The model required somewhat more attention to control because of a greater tendency to diverge in yaw which probably resulted from the decrease in directional stability (fig. 9).

The lateral-stability calculations indicate that the center-tail configuration should have had better oscillatory stability than the tip-tail configurations but the flight tests failed to show any appreciable differences in the behavior of the two configurations. Perhaps the need for continual control made it impossible to evaluate accurately the stability of the model in the higher lift range.

Vertical tails off.- Since one of the unusual characteristics of the canard airplane was the fact that it had static directional stability at high angles of attack with vertical tails off, an effort was made to study the dynamic behavior of the model in this configuration. Attempts to fly the model proved to be unsuccessful, however, because the model repeatedly yawed on take-off and crashed into the tunnel wall. This behavior was apparently caused by the fact that there was no rudder control to correct for the adverse yawing moments of the ailerons and the random changes in trim associated with the vortices from the tail. Also an important contributing factor to the model behavior was the negative damping in yaw at high angles of attack (see fig. 11).

The calculations show that the model was oscillatorily unstable over the entire lift-coefficient range with all vertical tails off.

[redacted]

CONCLUDING REMARKS

An investigation conducted in the Langley free-flight tunnel to determine the dynamic stability and control characteristics of a model of a canard-type airplane showed that the model characteristics were unsatisfactory in the higher lift-coefficient range. These unsatisfactory flight characteristics were caused by a reduction in lateral oscillatory stability as the lift coefficient increased and by an erratic behavior in pitch and yaw, apparently because of random trim changes associated with the flow from the horizontal tail.

Langley Aeronautical Laboratory,
National Advisory Committee for Aeronautics.
Langley Field, Va., August 26, 1953.

[redacted]

REFERENCES

1. Mathews, Charles W.: Study of the Canard Configuration With Particular Reference to Transonic Flight Characteristics and Low-Speed Characteristics at High Lift. NACA RM L8G14, 1949.

2. Crane, Harold L., and Adams, James J.: Wing-Flow Measurements of Longitudinal Stability and Control Characteristics of a Canard Airplane Configuration With a 45° Sweptback Wing and a Triangular All-Movable Control Surface. NACA RM L50A31, 1950.

3. Kraft, Christopher C., Jr., and Mathews, Charles W.: Determination by the Free-Fall Method of the Drag and Longitudinal Stability and Control Characteristics of a Canard Model at Transonic Speeds. NACA RM L50D04, 1950.

4. Bates, William R.: Low-Speed Static Longitudinal Stability Characteristics of a Canard Model Having a 60° Triangular Wing and Horizontal Tail. NACA RM L9H17, 1949.

5. Bates, William R.: Low-Speed Lateral Stability Characteristics of a Canard Model Having a 60° Triangular Wing and Horizontal Tail. NACA RM L9J12, 1949.

6. Draper, John W.: Low-Speed Static Stability Characteristics of a Canard Model With a 45° Sweptback Wing and a 60° Triangular Horizontal Control Surface. NACA RM L50G11, 1950.

7. Johnson, Joseph L., Jr.: Damping in Yaw and Static Directional Stability of a Canard Airplane Model and of Several Models Having Fuselages of Relatively Flat Cross Section. NACA RM L50H30a, 1950.

8. Johnson, Joseph L., Jr.: A Study of the Flow Field Behind the Triangular Horizontal Tail of a Canard Airplane at Approximately the Vertical-Tail Location by Means of a Tuft Grid. NACA RM L52H11, 1952.

9. Johnson, Joseph L., Jr.: A Study of the Use of Various High-Lift Devices on the Horizontal Tail of a Canard Airplane Model as a Means of Increasing the Allowable Center-of-Gravity Travel. NACA RM L52K18a, 1953.

10. Shortal, Joseph A., and Osterhout, Clayton J.: Preliminary Stability and Control Tests in the NACA Free-Flight Wind Tunnel and Correlation With Full-Scale Flight Tests. NACA TN 810, 1941.

[redacted]

11. MacLachlan, Robert, and Letko, William: Correlation of Two Experimental Methods of Determining the Rolling Characteristics of Unswept Wings. NACA TN 1309, 1947.

12. Campbell, John P., and McKinney, Marion O.: Summary of Methods for Calculating Dynamic Lateral Stability and Response and for Estimating Lateral Stability Derivatives. NACA Rep. 1098, 1952. (Supersedes NACA TN 2409.)

13. Letko, William, and Cowan, John W.: Effect of Taper Ratio on Low-Speed Static and Yawing Stability Derivatives of 45° Sweptback Wings With Aspect Ratio of 2.61. NACA TN 1671, 1948.

[redacted]

TABLE I.- MASS AND DIMENSIONAL CHARACTERISTICS OF MODEL

Weight, lb	18.5
Wing loading, W/S, lb/sq ft	3.47
Mass density factor μ	11.32
Moments of inertia:	
I_X, slug-ft^2	0.243
I_Y, slug-ft^2	0.94
I_Z, slug-ft^2	1.13
Wing:	
Airfoil section	NACA 0012
Area, sq ft	5.33
Span, ft	4.0
Aspect ratio	3.0
Incidence, deg	0
Dihedral, deg	0
Root chord, ft	1.77
Taper ratio	0.5
Mean aerodynamic chord, ft	1.383
Aileron area, sq ft (2 ailerons)	0.514
Tip tails:	
Airfoil section	NACA 0009
Area, sq ft (2 tails)	0.533
Span, ft	0.62
Root chord, ft	0.562
Taper ratio	0.50
Aspect ratio	1.49
Rudder area, percent tail area	30
Tail length, ft (center of gravity to leading edge of tip-tail root chord)	1.78
Center tail:	
Airfoil section	NACA 0009
Area, sq ft	0.272
Span, ft	0.73
Root chord, ft	0.495
Taper ratio	0.505
Aspect ratio	1.96
Rudder area, percent tail area	38.4
Tail length, ft (center of gravity to leading edge of tip-tail root chord)	1.94

TABLE I.- MASS AND DIMENSIONAL CHARACTERISTICS OF MODEL - Concluded

Horizontal tail (triangular):	
Airfoil section	Flat plate
Area, sq ft	0.80
Span, ft	1.36
Sweepback, of leading edge, deg	60
Aspect ratio	2.31
Horizontal tail (sweptback)	
Airfoil section	NACA 0012
Area, sq ft	0.80
Span, ft	1.54
Sweepback, of leading edge, deg	45
Aspect ratio	2.97
Leading-edge flap deflection, deg	65
Flap chord, percent of chord of tail	17

TABLE II.- RESULTS OF CALCULATIONS TO DETERMINE THE PERIOD AND TIME TO DAMP TO ONE-HALF AMPLITUDE OF THE FLIGHT-TEST MODEL

Condition	α, deg	C_L	$\left(\frac{k_X}{b}\right)^2$	$\left(\frac{k_Z}{b}\right)^2$	i_t, deg	K_X^2	K_Z^2	K_{XZ}	Tan γ	μ_b	$\frac{m}{\rho S V}$	C_{l_p}	C_{n_p}	C_{Y_p}	C_{l_r} (a)	C_{n_r} (b)	C_{Y_r} (c)	C_{l_β}	C_{n_β}	C_{Y_β}	Oscillatory mode		Aperiodic mode	
																					Period, sec	$T_{1/2}$, sec	Rolling, $T_{1/2}$, sec	Spiral, $T_{1/2}$, sec
Wing-tip tails	9.5	0.4	0.0264	0.124	8.5	0.0285	0.1219	0.0143	-0.1800	11.32	0.529	-0.23	-0.045	0.25	0.163	-0.125	0.180	-0.195	0.098	-0.258	1.120	1.920	0.156	6.22
	17.0	0.8	.0264	.124	16.0	.0338	.1166	.0259	-.2375	11.32	.749	-.18	-.030	.29	.067	.050	.150	-.137	.194	-.287	1.160	-10.000	.280	-10.00
	22.0	1.0	.0264	.124	21.0	.0389	.1115	.0327	-.3500	11.32	.839	-.12	.025	.23	-.008	.240	.200	-.057	.235	-.229	1.230	-1.320	.437	20.80
Wing-tip tails plus center tail	9.5	0.4	.0264	.124	8.5	.0285	.1219	.0143	-.1800	11.32	.529	-.24	-.060	.31	.169	-.360	.340	-.195	.183	-.413	0.927	0.786	.161	2.57
	17.0	0.8	.0264	.124	16.0	.0338	.1166	.0259	-.2375	11.32	.749	-.17	-.075	.54	.083	-.390	.120	-.137	.172	-.258	1.180	1.430	.305	2.06
	22.0	1.0	.0264	.124	21.0	.0389	.1115	.0327	-.3500	11.32	.839	-.11	-.050	.58	.016	-.420	.029	-.057	.103	-.069	1.670	2.310	.540	1.05
																			[d].515	[d]-.460	[d]1.090	[d]1.230	[d].485	[d]5.07
Center tail	9.5	0.4	.0264	.124	8.5	.0285	.1219	.0143	-.1800	11.32	.529	-.22	-.080	.34	.166	-.200	.210	-.195	.057	-.287	1.110	2.730	.157	2.80
	17.0	0.8	.0264	.124	16.0	.0338	.1166	.0259	-.2375	11.32	.749	-.15	-.005	.41	.090	-.300	-.090	-.137	.057	-.057	1.650	2.180	.395	0.99
	22.0	1.0	.0264	.124	21.0	.0389	.1115	.0327	-.3500	11.32	.839	-.09	.010	.44	.026	-.460	-.230	-.066	-.057	.185	4.202 9.27	-.870 .335	---	---
																			[d].150	[d]-.400	[d]1.500	[d]1.070	[d].680	[d]1.19
Vertical tails off	9.5	0.4	.0264	.124	8.5	.0285	.1219	.0143	-.1800	11.32	.529	-.21	-.065	.28	.187	0	0	-.195	-.006	-.086	1.440	-2.690	.154	10.88
	17.0	0.8	.0264	.124	16.0	.0338	.1166	.0259	-.2375	11.32	.749	-.16	.040	.16	.083	.100	0	-.137	.086	-.143	1.480	-31.200	.308	-3.13
	22.0	1.0	.0264	.124	21.0	.0389	.1115	.0327	-.3500	11.32	.839	-.10	.090	.09	.016	.200	0	-.057	.115	-.029	1.640	-1.850	.435	-3.26

[a] $C_{l_{r_{tail}}} = -2\frac{l}{b}C_{l_{\beta_{tail}}}$.

[b] $C_{n_{r_{tail}}} = 2\left(\frac{l}{b}\right)^2 C_{Y_{\beta_{tail}}}$.

[c] $C_{Y_{r_{tail}}} = -2\frac{l}{b}C_{Y_{\beta_{tail}}}$.

[d] Obtained for $\beta > \pm 5°$.

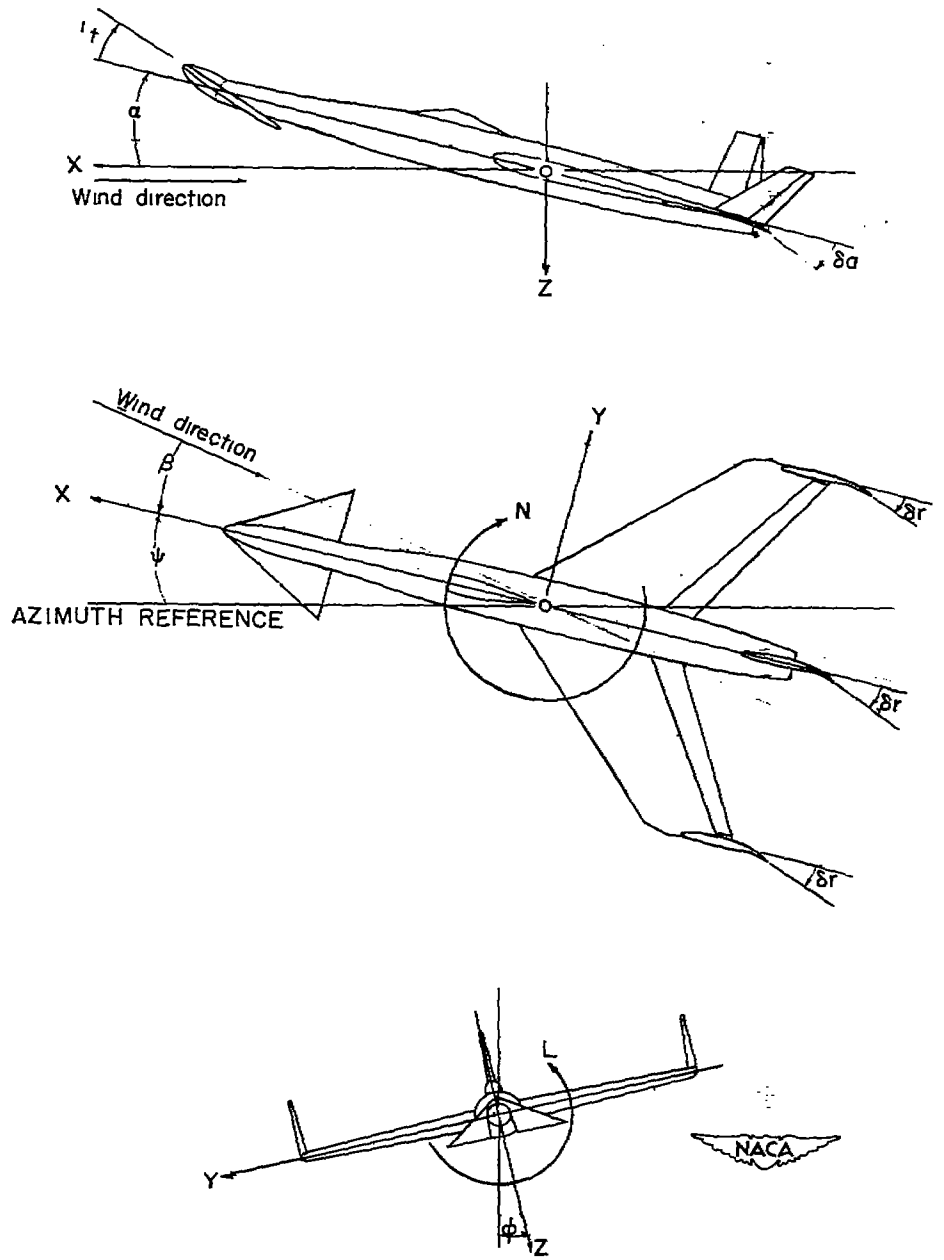

Figure 1.- The stability system of axes. Arrows indicate positive directions of moments, forces, and angles. This system of axes is defined as an orthogonal system having the origin at the center of gravity and in which the Z-axis is in the plane of symmetry and perpendicular to the relative wind, the X-axis is in the plane of symmetry and perpendicular to the Z-axis, and the Y-axis is perpendicular to the plane of symmetry. At a constant angle of attack, these axes are fixed in the airplane.

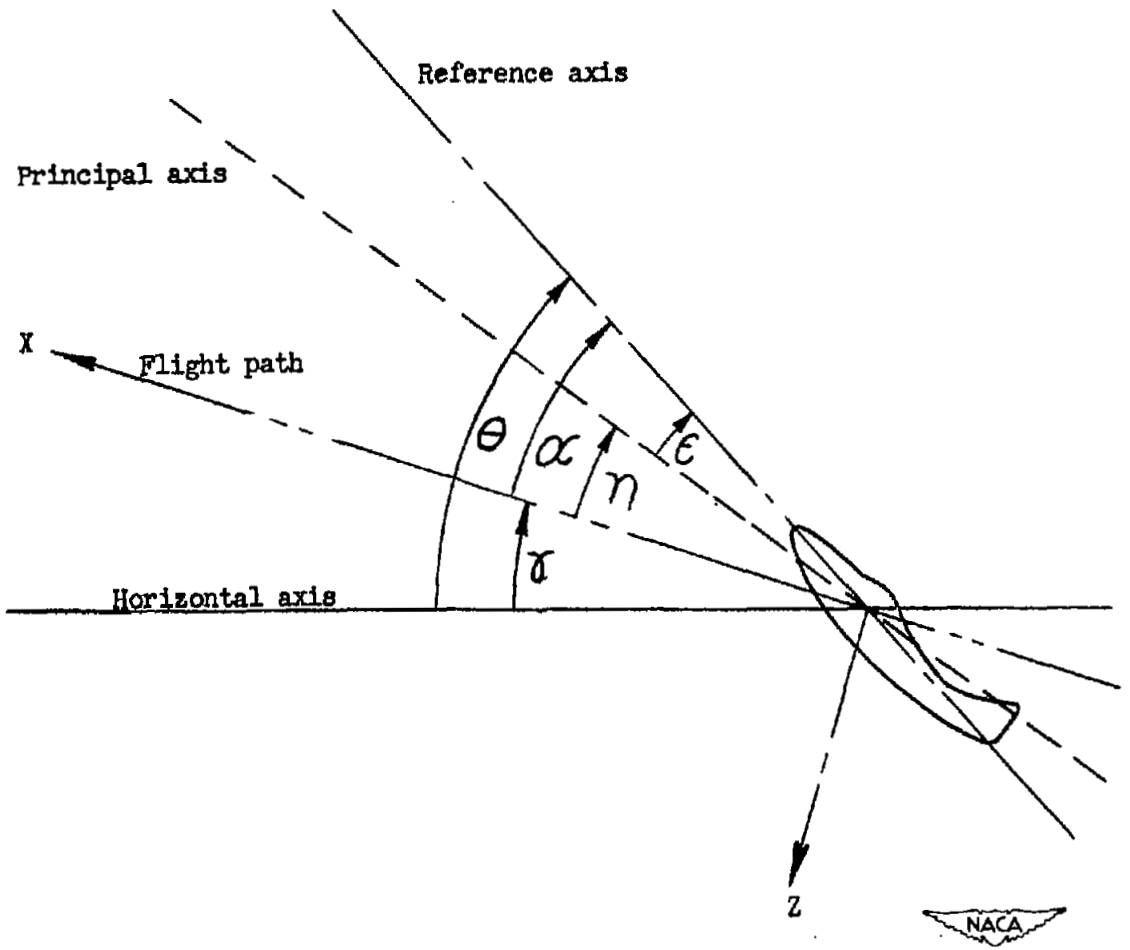

Figure 2.- System of axes and angular relationship in flight. Arrows indicate positive direction of angles. $\eta = \theta - \gamma - \epsilon$.

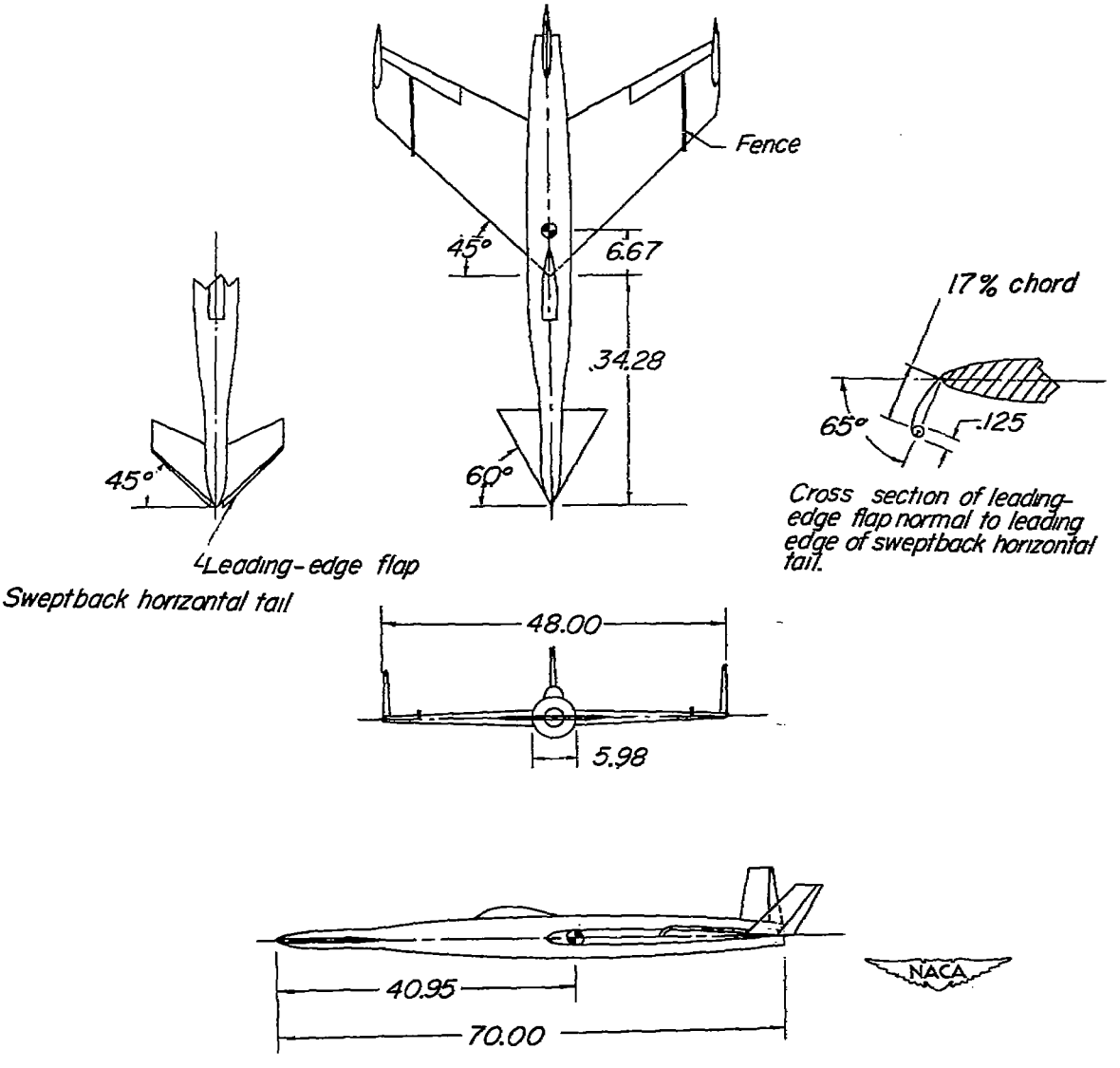

Figure 3.- Three-view drawing of canard model used in the free-flight-tunnel investigation. All dimensions are in inches.

L-62374

Figure 4.- Model tested in the Langley free-flight tunnel.

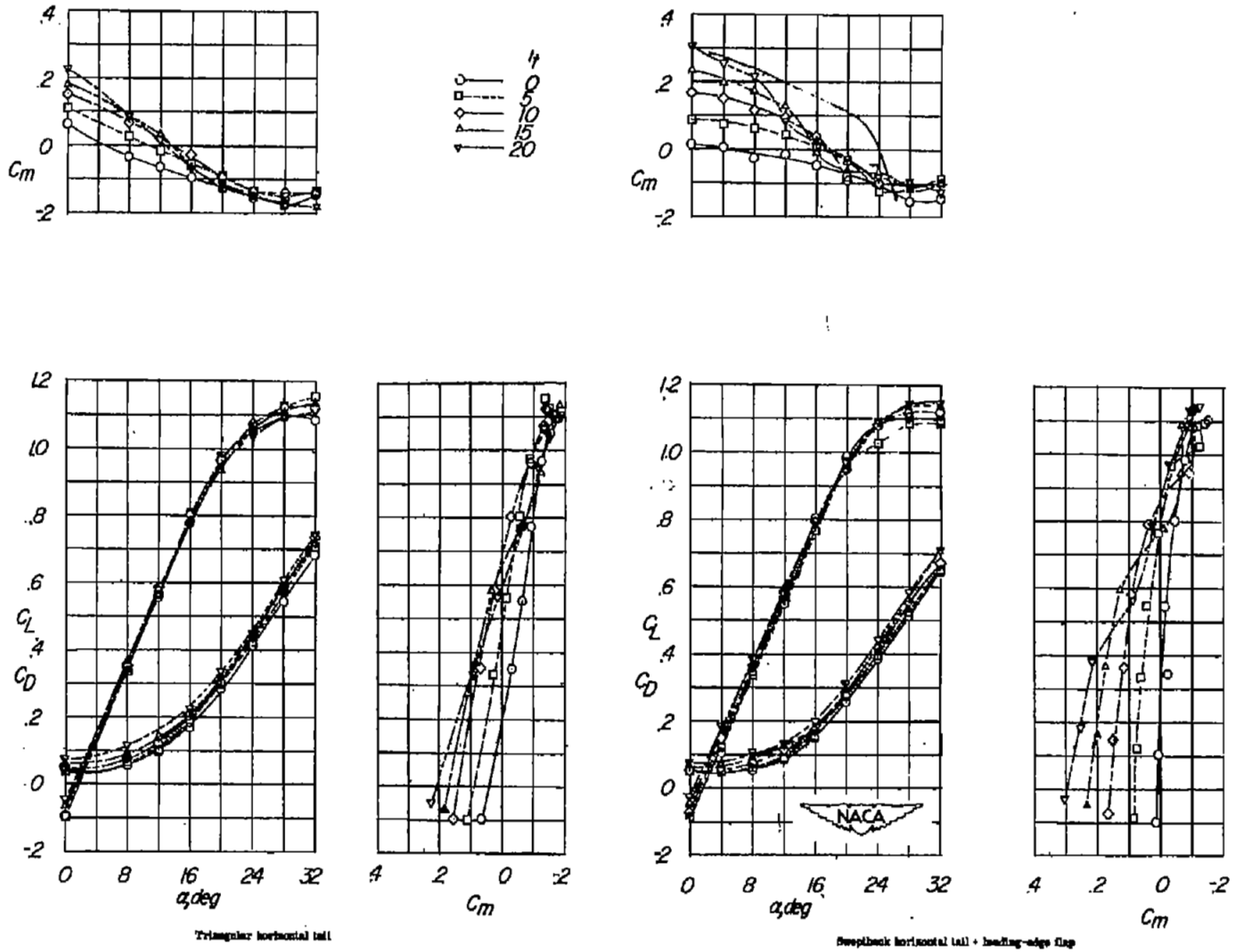

Figure 5.- Longitudinal characteristics of the model. $\beta = 0^{\circ}$.

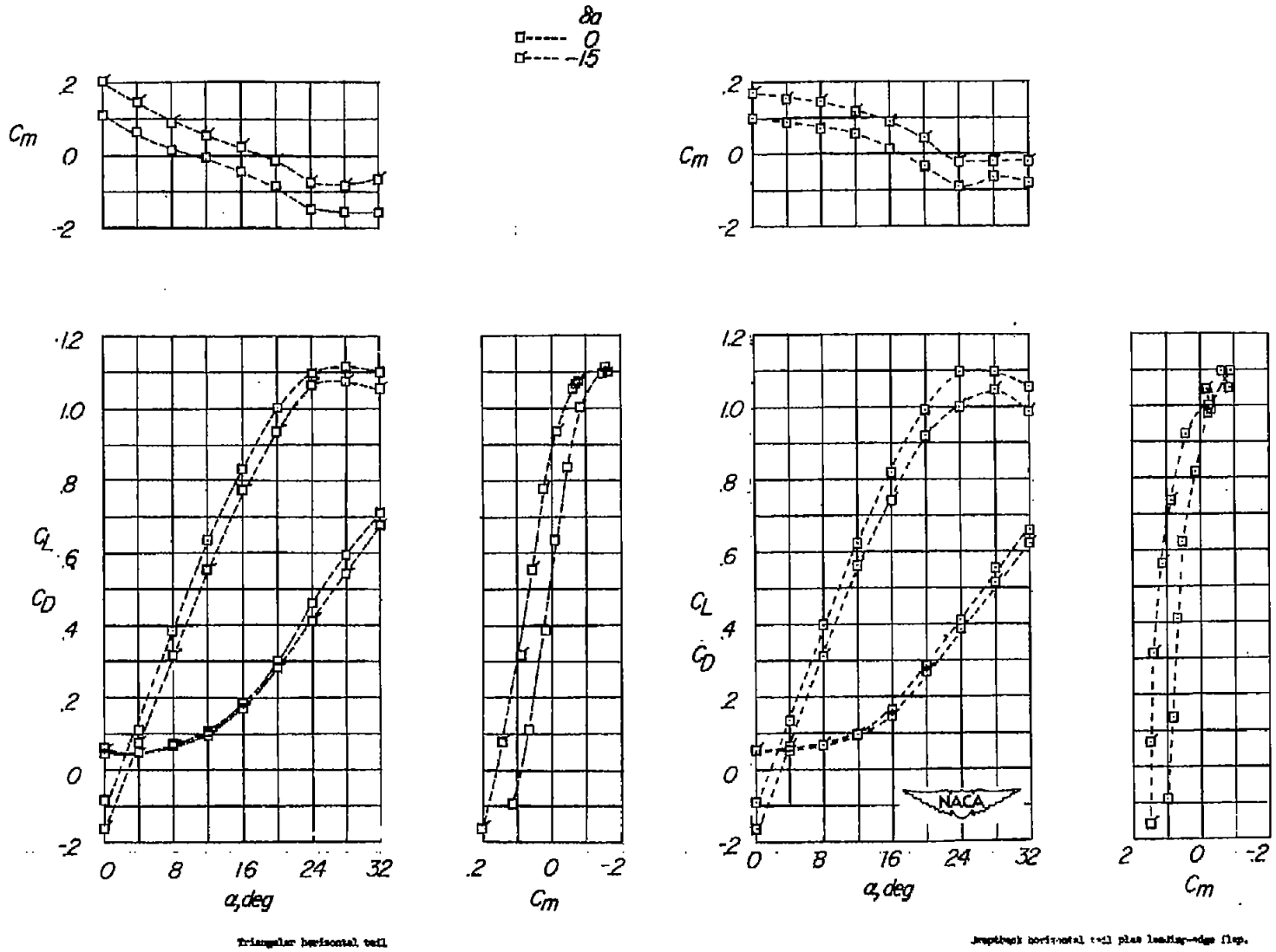

Figure 6:- Effect of deflection of ailerons as trimmers on the longitudinal characteristics of model. $\beta = 0^{\circ}$; $i_t = 5^{\circ}$.

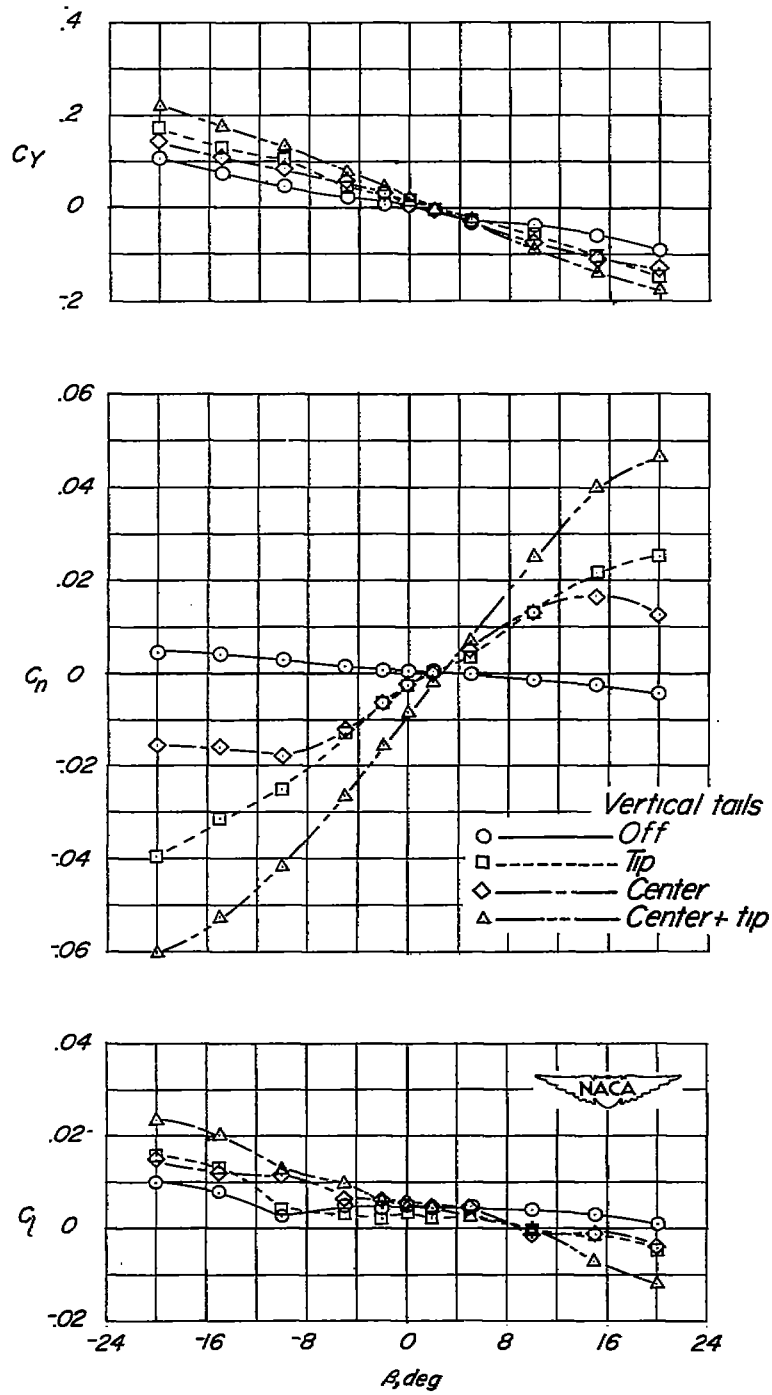

(a) $\alpha = 0^\circ$.

Figure 7.- Lateral characteristics of model with triangular horizontal tail. $i_t = 5^\circ$; both ailerons deflected -15°.

[redacted]

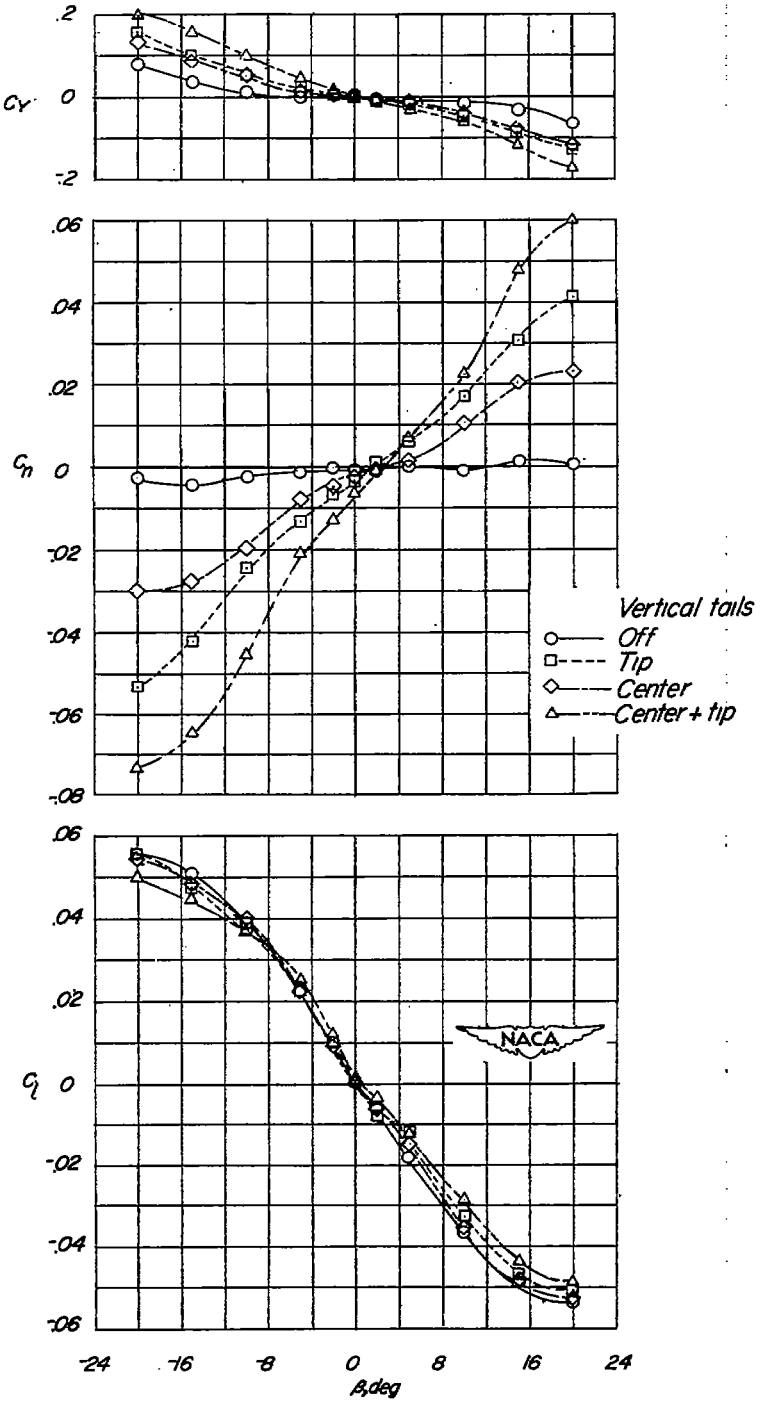

(b) $\alpha = 12^{\circ}$.

Figure 7.- Continued.

[redacted]

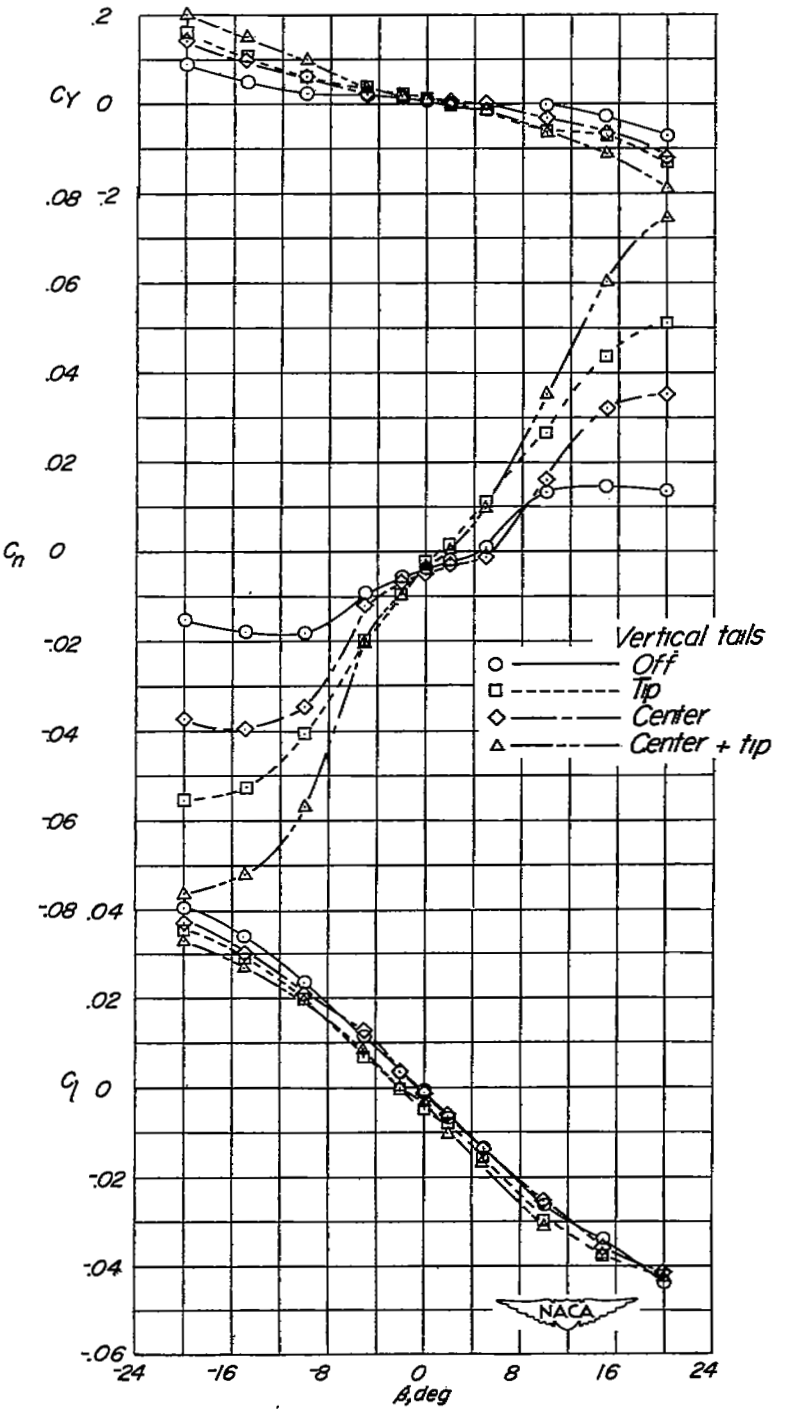

(c) $\alpha = 16^\circ$.

Figure 7.- Continued.

[redacted]

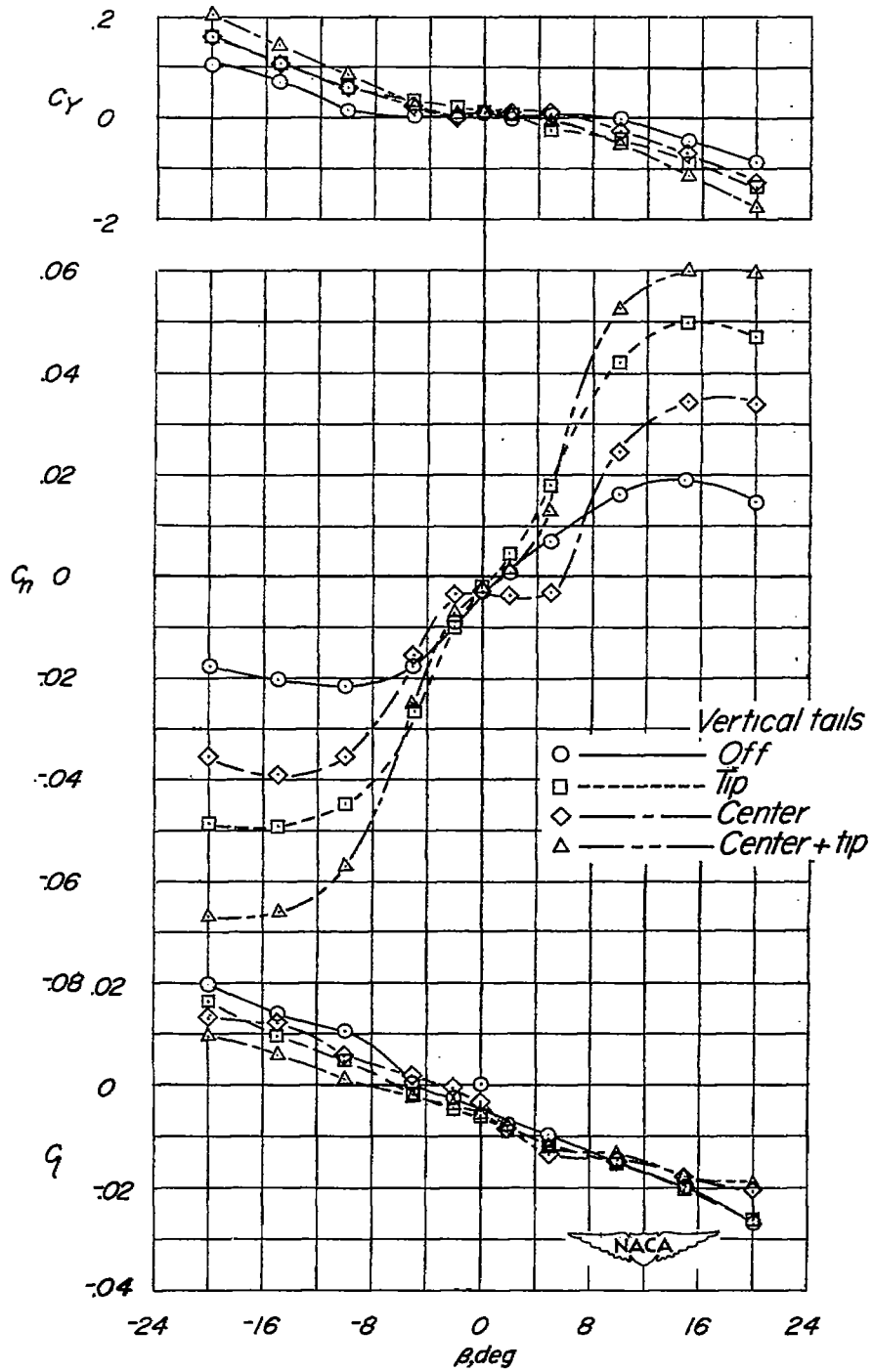

(d) $\alpha = 20^{\circ}$.

Figure 7.- Continued.

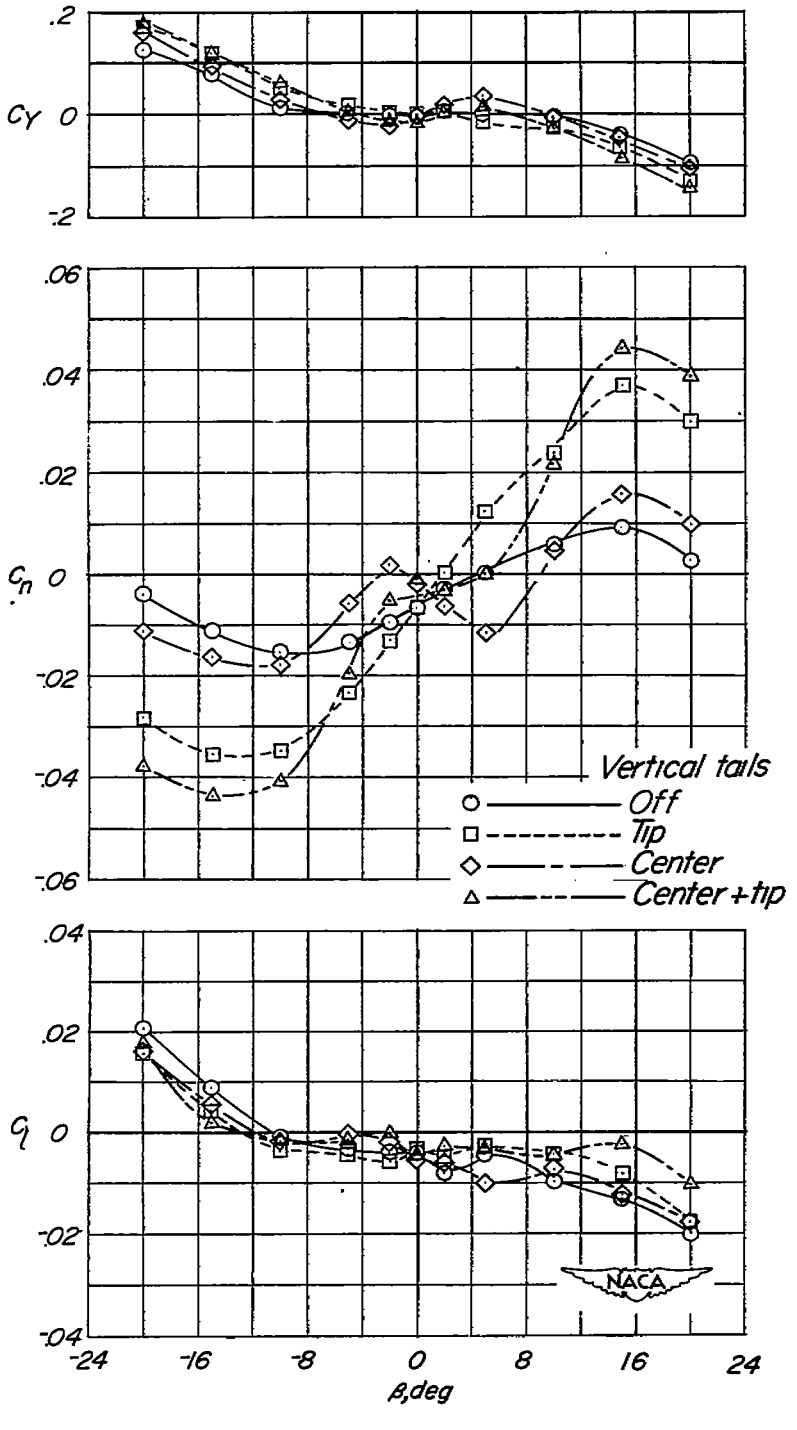

(e) $\alpha = 24^{\circ}$.

Figure 7.- Concluded.

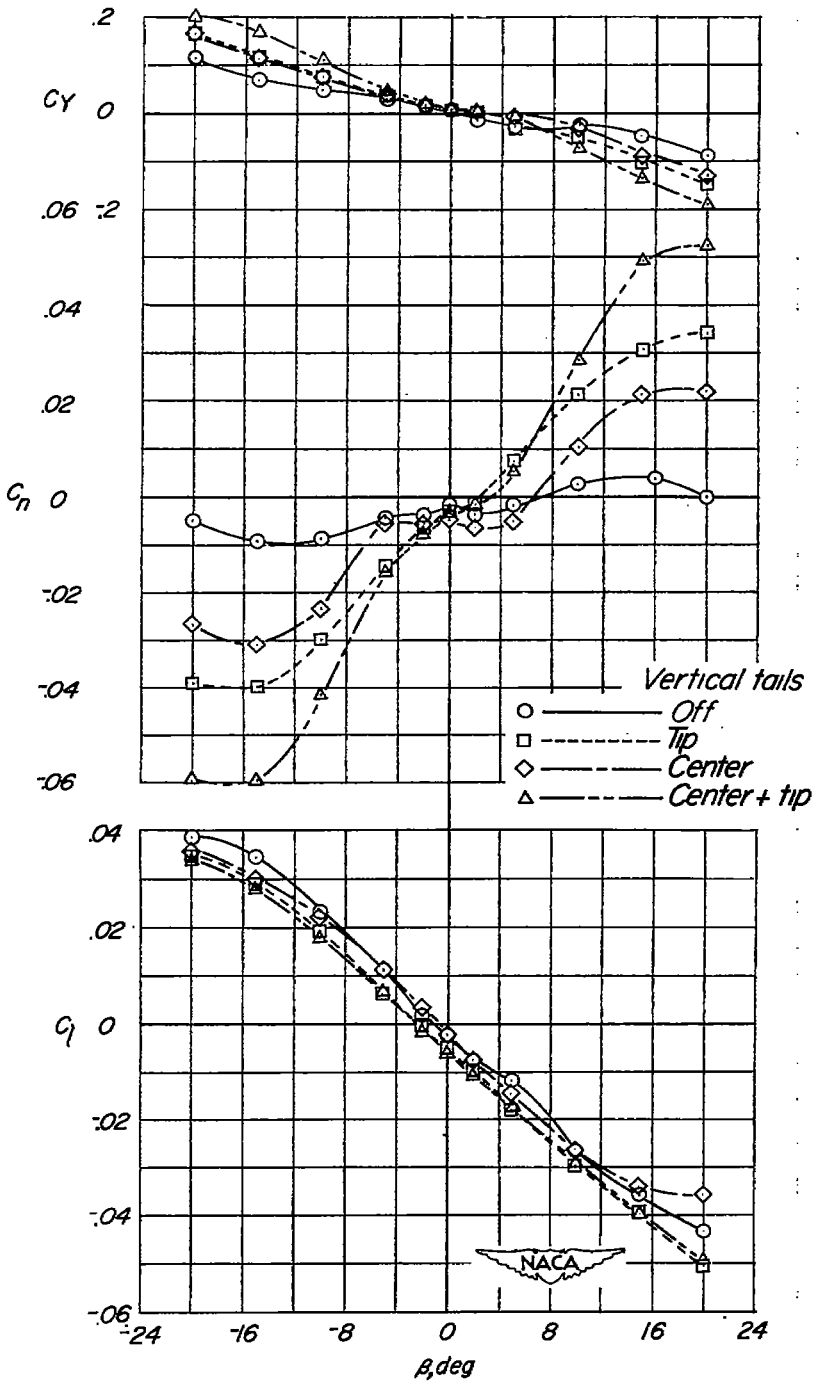

(a) $\alpha = 16^\circ$.

Figure 8.- Lateral characteristics of model with sweptback horizontal tail plus leading-edge flap. $i_t = 5^\circ$; both ailerons deflected -15°.

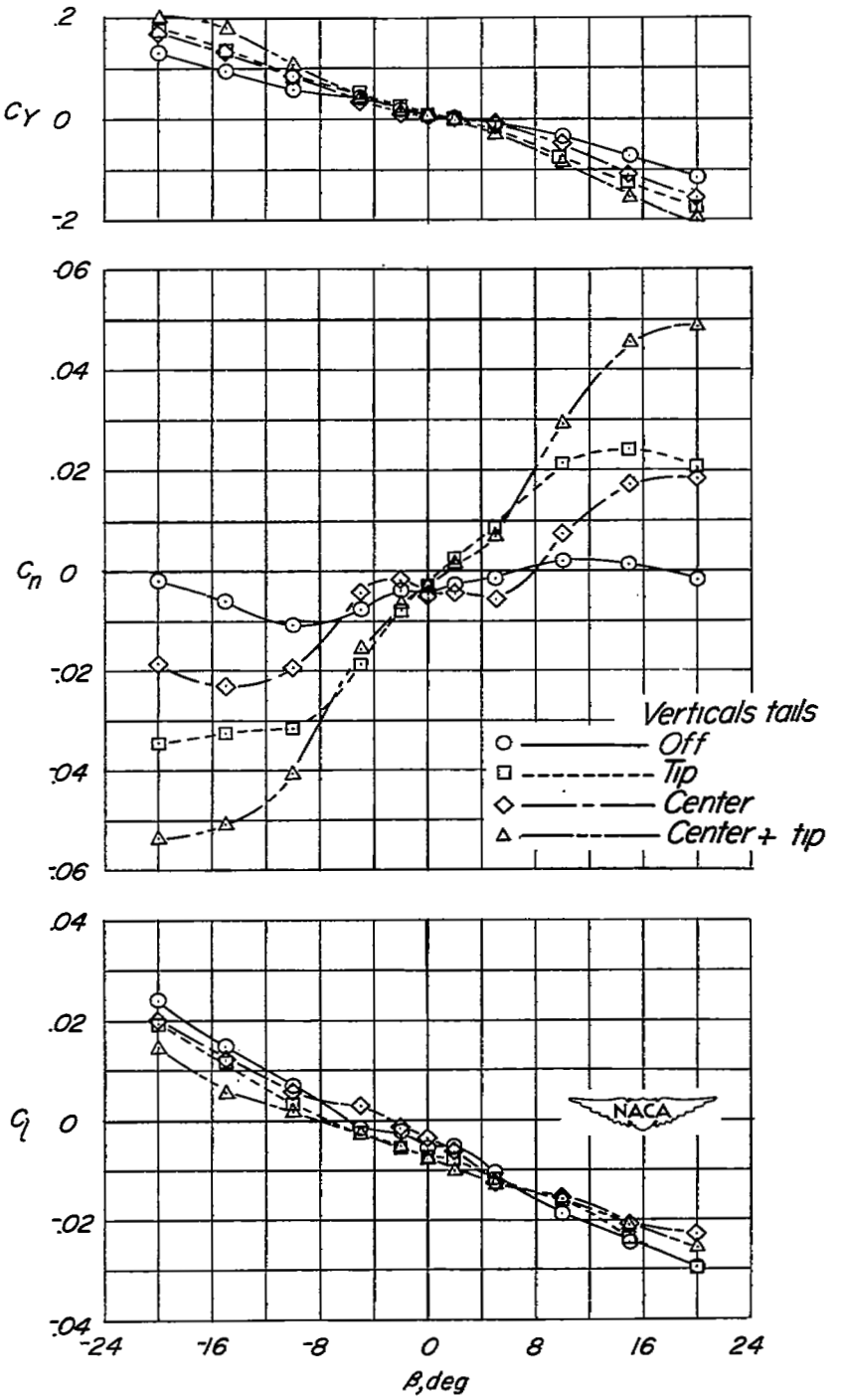

(b) $\alpha = 20^\circ$.

Figure 8.- Continued.

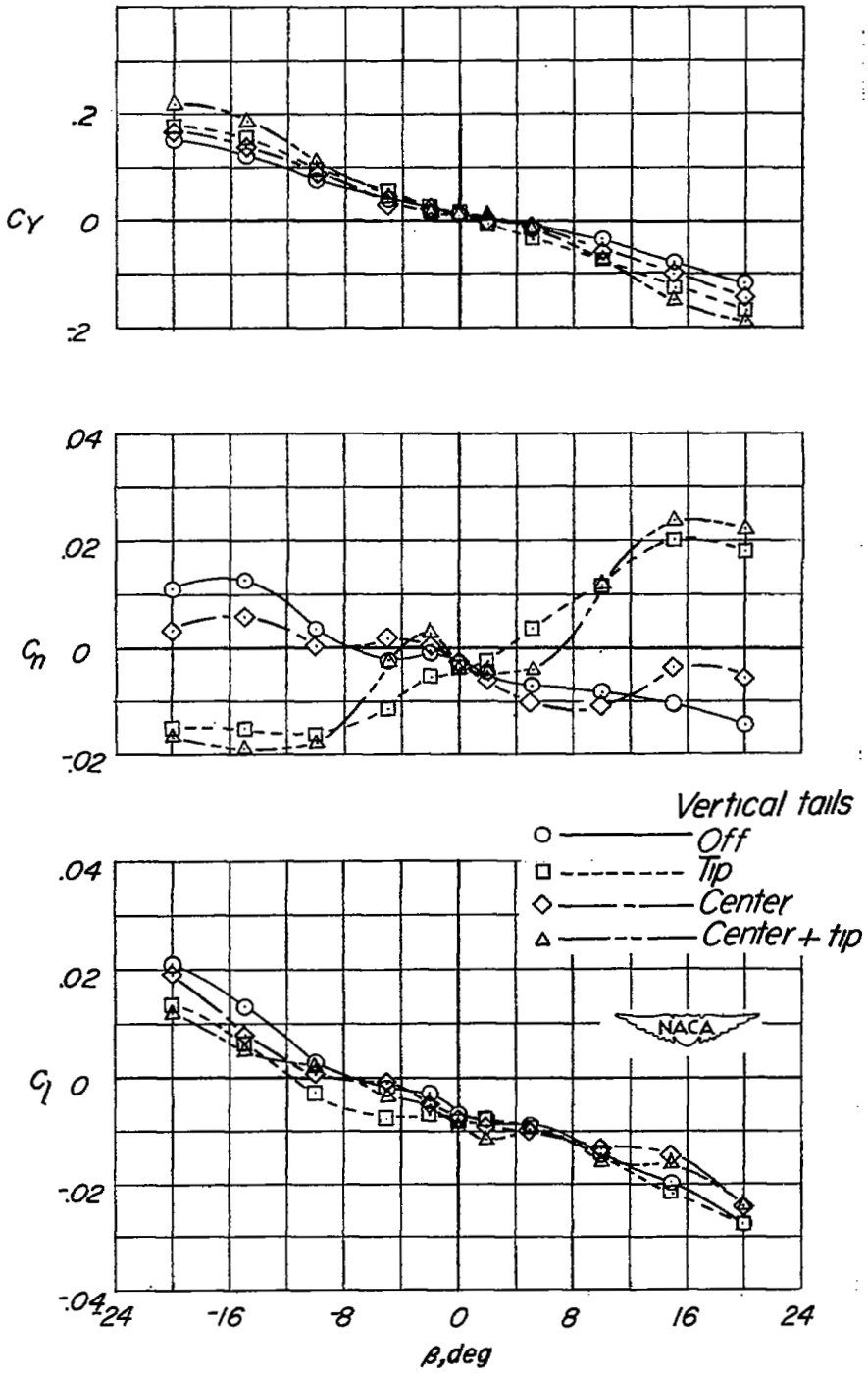

(c) $\alpha = 24°$.

Figure 8.- Concluded.

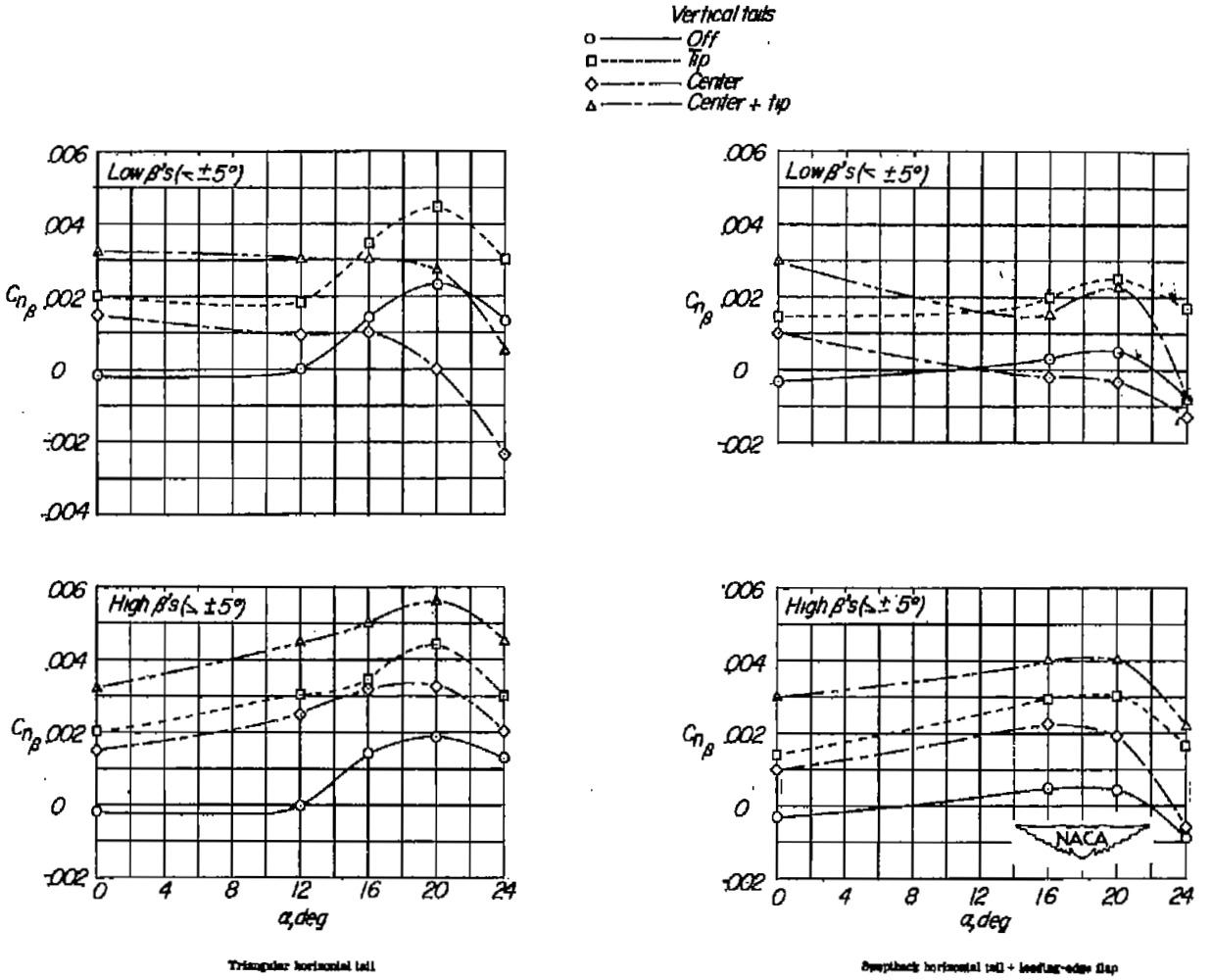

Figure 9.- Effect of vertical tail configuration on directional stability parameter at low and high angles of sideslip. $i_t = 5^\circ$; both ailerons deflected -15°.

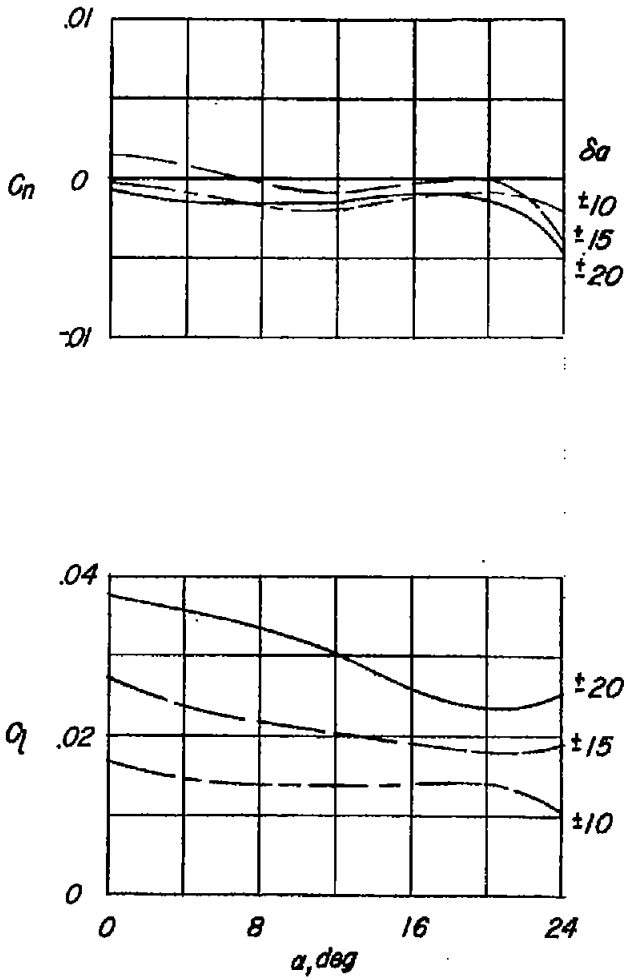

(a) Aileron effectiveness.

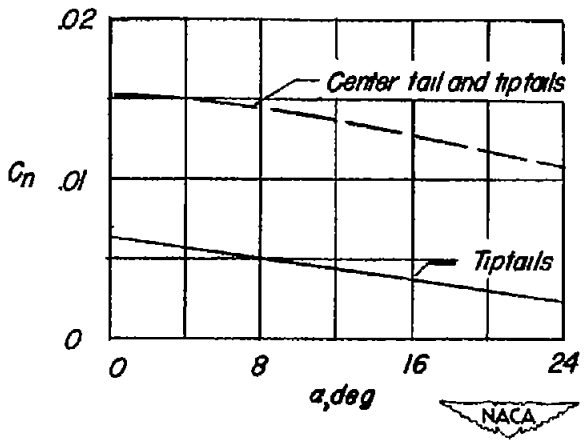

(b) Rudder effectiveness, $\delta_r = 10^\circ$ right.

Figure 10.- Control characteristics of model. $i_t = 5^\circ$; both ailerons at a trim setting of -15°.

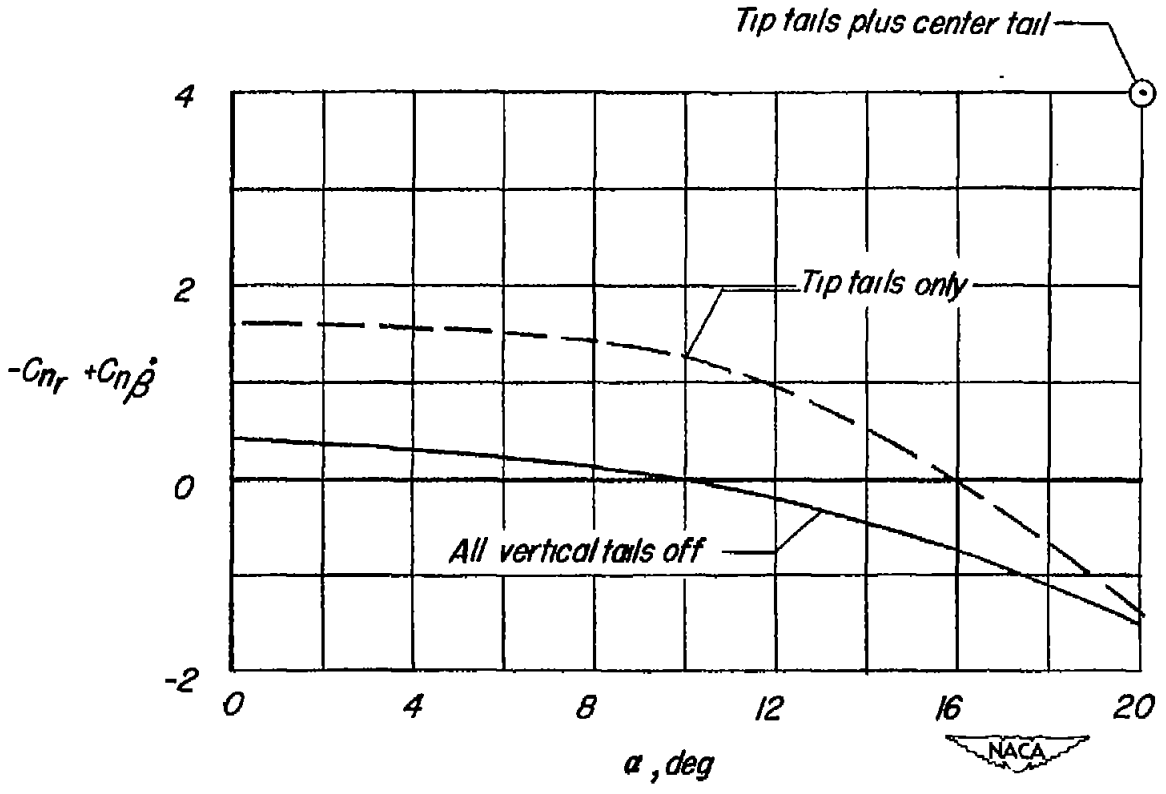

Figure 11.- Damping-in-yaw characteristics of model with triangular horizontal tail. $i_t = 10^\circ$; $\delta_a = 0^\circ$. (Data from ref. 7.)

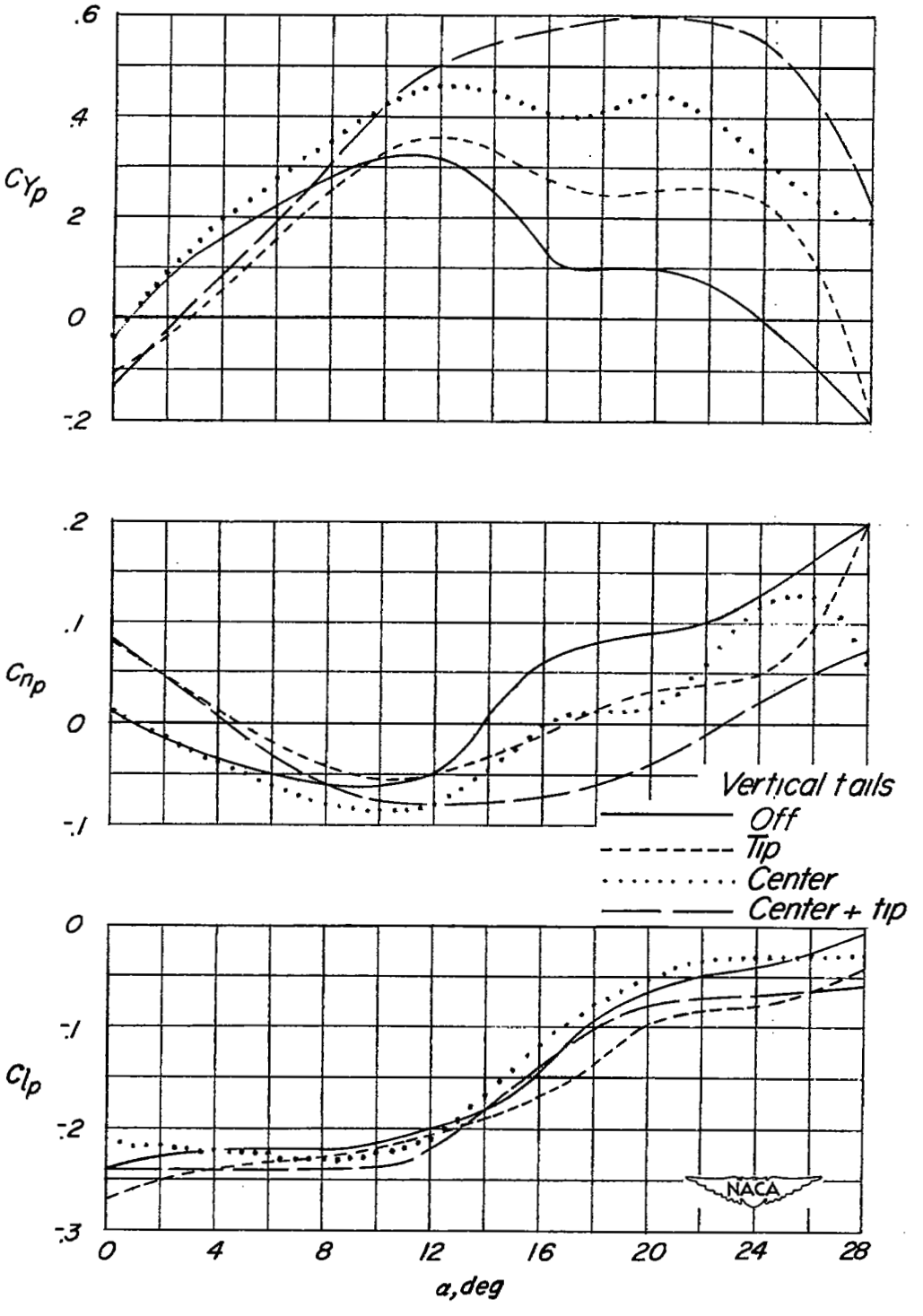

Figure 12.- Rotary derivatives of model with triangular horizontal tail. $i_t = 5°$; both ailerons deflected -15°.

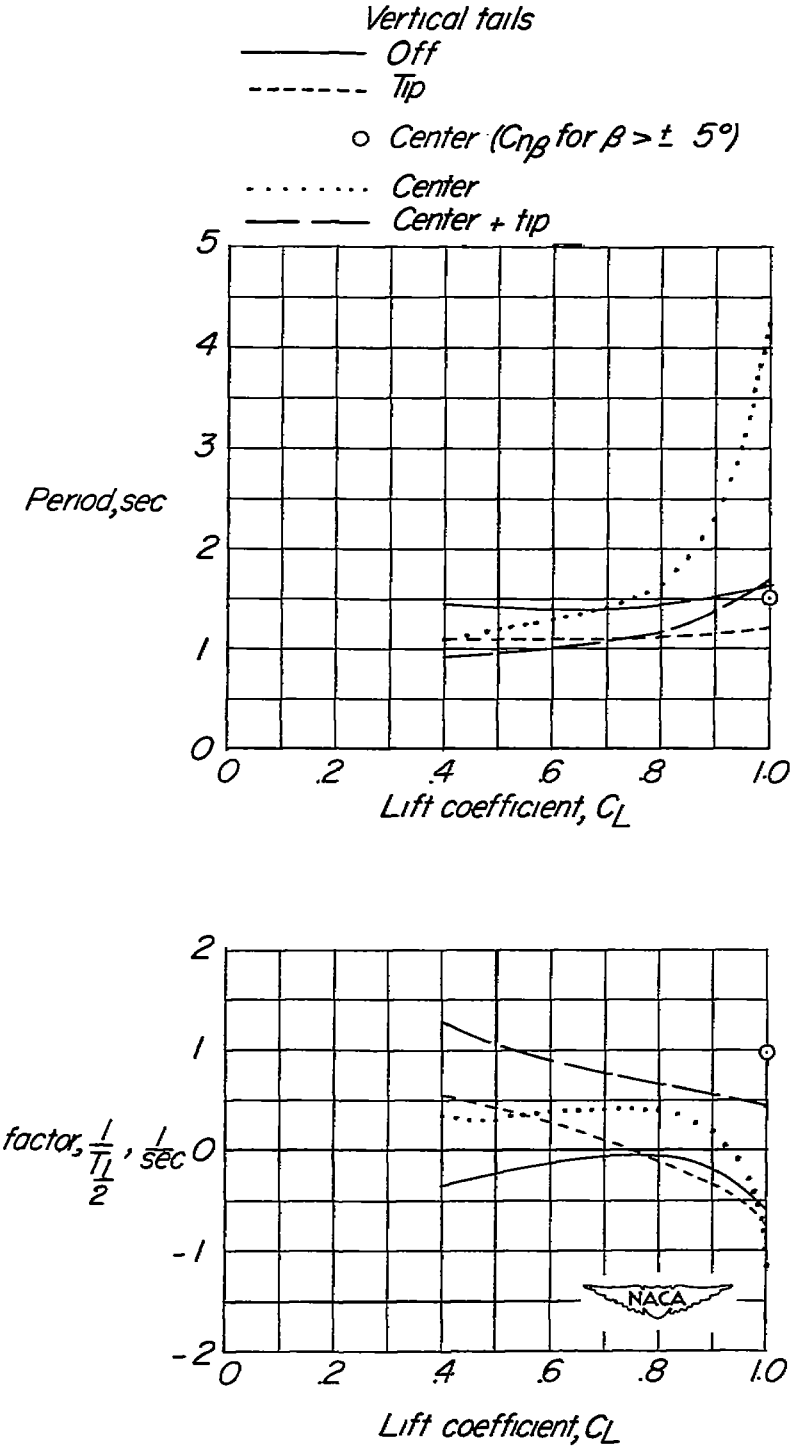

Figure 13.- Calculated damping and period characteristics of model. Static derivatives obtained for $\beta < \pm 5^\circ$ except as noted.

NACA-Langley - 10-29-53 - 325